Talanta 115 (2013) 40–46

Contents lists available at ScienceDirect

Talanta

journal homepage: www.elsevier.com/locate/talanta

Solubility of hot fuel particles from Chernobyl—Influencing parameters for individual radiation dose calculations

Evgenii K. Garger [a], Oliver Meisenberg [b,*], Oleksiy Odintsov [a], Viktor Shynkarenko [a], Jochen Tschiersch [b]

[a] Institute for Safety Problems of Nuclear Power Plants of the National Academy of Sciences, Ukraine, Lysogorskaya 12, Building 106, 03028 Kiev, Ukraine
[b] Helmholtz Zentrum München, German Research Center for Environmental Health, Institute of Radiation Protection, Ingolstädter Landstr. 1, 85764 Neuherberg, Germany

ARTICLE INFO

Article history:
Received 14 November 2012
Received in revised form
28 March 2013
Accepted 8 April 2013
Available online 15 April 2013

Keywords:
Solubility kinetics
Nuclear fuel
Simulated lung fluid
Inhalation dose
Chernobyl

ABSTRACT

Nuclear fuel particles of Chernobyl origin are carriers of increased radioactivity (hot particles) and are still present in the atmosphere of the Chernobyl exclusion zone. Workers in the zone may inhale these particles, which makes assessment necessary. The residence time in the lungs and the transfer in the blood of the inhaled radionuclides are crucial for inhalation dose assessment. Therefore, the dissolution of several kinds of nuclear fuel particles from air filters sampled in the Chernobyl exclusion zone was studied. For this purpose filter fragments with hot particles were submersed in simulated lung fluids (SLFs). The activities of the radionuclides ^{137}Cs, ^{90}Sr, $^{239+240}$Pu and ^{241}Am were measured in the SLF and in the residuum of the fragments by radiometric methods after chemical treatment. Soluble fractions as well as dissolution rates of the nuclides were determined. The influence of the genesis of the hot particles, represented by the ^{137}Cs/$^{239+240}$Pu ratio, on the availability of ^{137}Cs was demonstrated, whereas the dissolution of ^{90}Sr, $^{239+240}$Pu and ^{241}Am proved to be independent of genesis. No difference in the dissolution of ^{137}Cs and $^{239+240}$Pu was observed for the two applied types of SLF. Increased solubility was found for smaller hot particles. A two-component exponential model was used to describe the dissolution of the nuclides as a function of time. The results were applied for determining individual inhalation dose coefficients for the workers at the Chernobyl construction site. Greater dose coefficients for the respiratory tract and smaller coefficients for the other organs were calculated (compared to ICRP default values). The effective doses were in general lower for the considered radionuclides, for ^{241}Am even by one order of magnitude.

1. Introduction

Following a nuclear accident with a release of fragments of the nuclear fuel matrix, so-called hot nuclear fuel particles contribute a significant amount to the inhalation dose [1]. There are many studies about various aspects of the release of radioactive material and hot particles from the Chernobyl reactor accident. They include a classification of the emitted products taking into consideration the chemical and nuclear-physical characteristics of the released material [2–7]. Airborne fuel particles were detected in filter samples after long range transport [8] and in resuspended material in the Chernobyl area [9]. As these particles are still present in the atmosphere of the Chernobyl area, workers in the exclusion zone e.g. for construction of the new shelter may inhale these particles and dose assessment for this group of population is required. For this purpose deposition and absorption of airborne radionuclides in the respiratory tract must be quantified. Besides activity concentration and particle size, the solubility of the aerosol particles which contain the radionuclides is the determining parameter. Although several solubility studies with application to radioactively contaminated aerosol exist, there are only a few studies devoted to the solubility in the atmospheric aerosol of Chernobyl origin [10–13].

This work presents the dissolution characteristics for the radionuclides ^{137}Cs, ^{90}Sr, $^{239+240}$Pu and ^{241}Am from hot airborne particles in two frequently used types of simulated lung fluid (SLF) [14] in a large number of samples (37 in total). The airborne fuel particles were sampled inside the Chernobyl Shelter and at several locations in its vicinity. Applying the Human Respiratory Tract Model of the International Commission on Radiological Protection (ICRP) [15] the inhalation dose coefficients were calculated specifically for the workers at the new shelter of the Chernobyl Nuclear Power Plant.

2. Materials and methods

2.1. Sampling

Radioactive aerosol was sampled for more than two decades at different sites of the 30 km exclusion zone of the Chernobyl

* Corresponding author. Tel.: +49 89 3187 2203; fax: +49 89 3187 3323.
E-mail addresses: egarger@mail.ru (E.K. Garger), oliver.meisenberg@helmholtz-muenchen.de (O. Meisenberg), aaodin@mail.ru (O. Odintsov), shvk@ua.fm (V. Shynkarenko), tschiersch@helmholtz-muenchen.de (J. Tschiersch).

0039-9140/$ - see front matter © 2013 Elsevier B.V. All rights reserved.
http://dx.doi.org/10.1016/j.talanta.2013.04.021

Table 1
Sampling scenarios at ChNPP and in its vicinity.

Sample type	Scenario	Sampling site and distance to the Shelter	Date	Sampler	Type of filter
1	Inside Shelter	Room 406/2 (level +12.5 m)	20–30.10.2002	PM-10 impactor	Fiberglass
2	Gap in the Shelter	Machine hall	03–15.10.2002	SES	Fiberglass
3	Near-field zone	Southern vicinity of the Shelter, 50 m	16–21.11.2001	Grad	Petryanov cloth
4	Far-field zone	City of Pripyat, 4 km	23–24.08.1988, 09.–10.05.1988	Typhoon	Petryanov cloth

nuclear power plant (ChNPP) [16]. A part of these aerosol samples was used for the physico-chemical analysis of the aerosol particles. In Table 1 information about sites and time of sampling, samplers and filter material is presented.

The samples were classified according to characteristic places and the scenario of sampling. Samples of type 1 were taken in room 406/2, which is used for the preparation of scientific experiments, inside the Shelter. The sampler for samples of type 2 was set up in a gap of the Shelter close to the southern wall of the former machine hall. Samples of type 3 were taken in the southern proximity at a distance of 50 m from the Shelter. The sampler of type 4 was situated in the city of Pripyat about 4 km west of ChNPP. The sampling in the gaps of the Shelter was conducted with a portative sampler SES (Institute of Radioecology, Ukraine), with a flow rate of 70 m^3/h and Whatman filters 441 (0.20×0.30 m^2). The sampling in the proximity of the Shelter was conducted with a sampler Grad (SPA Typhoon, Russia, 400 m^3/h) with Petryanov filters (perchlorvinyl resin fibers, 0.77×0.34 m^2). An Andersen cascade impactor PM 10 (Andersen, USA, six stages, 67.8 m^3/h) was used for size-classified aerosol sampling in room 406/2.

In general higher activity concentrations were measured in the southern vicinity of the Shelter, which is the lee side for most weather conditions, than at other places around the Shelter. The pronounced maximum of the airborne activity concentrations was reached in the period 14–21.11.2001 with 142 mBq/m^3 for ^{137}Cs, 115 mBq/m^3 for ^{90}Sr and 3.55 mBq/m^3 for $^{239+240}$Pu. Therefore, the data from the samples of type 3 can provide a conservative estimate of the inhalation exposure for the workers at the Shelter site.

2.2. Autoradiography

Autoradiographical examinations of the aerosol samples were conducted with use of a medical X-ray film of high sensitivity (CP-BU-new, Agfa) [13]. The autoradiographical images of the filters were taken inside cartridges, in which the filters were protected by membrane filters and covered on both sides by the film. Depending on the activity of the fragments the exposure time varied between 14 and 35 days. Digital images of the recorded autoradiograms were gained with the help of the scanner Epson Perfection-1670. Diameters of hot spots at a given threshold of blackening and their aggregate optical density were measured with the image processing package Image-Pro Plus 5.0 (Media Cybernetics).

Additional to the exposure of the filter samples, an autoradiogram of several different hot particles with known activity was recorded. This made possible the calibration of autoradiography measurements to the activity of the hot particles and thus determination of the activity of individual particles on the filters [13,17]. With the known specific activity A_{spec} of the irradiated nuclear fuel matrix of ChNPP, the particle volume and volume equivalent diameter (i.e. the diameter of a spherical particle with the volume as that of the considered particle) can be calculated as well; $A_{spec} = 2.5 \times 10^9$ Bq/g (mainly from ^{137}Cs, ^{90}Sr and ^{90}Y) for 2005 when the autoradiography was done [10]. With the volume equivalent particle diameter d_e the aerodynamic diameter d_{ae} of the hot particles can be calculated according to [18], which neglects particle shape and slip correction, as

$$d_{ae} \approx d_e(\rho/1\ \mathrm{g/cm^3})^{1/2} \quad (1)$$

with $\rho = 10.4$ g/cm³ as the density of Chernobyl hot particles [19]. In contrast to this method, samples of type 1 (sampling inside the Shelter) were taken using a cascade impactor. For these samples, the sampling characteristics of the impactor yield a size range for the aerodynamic diameter of the hot particles.

2.3. Selection of filter fragments for the dissolution experiments

With the help of the autoradiograms, regions on the filters which contained either several hot particles of similar size or single large hot particles were identified and cut out. The gained fragments had diameters of 48 mm for those with several hot particles and of 8 mm for those with single hot particles (Fig. 1). The total alpha and beta activities of the fragments were measured with a low background alpha/beta radiometer Canberra IN-20. After these measurements several of the small filter fragments, each of one group of the same filter, were selected according to their activity and fixed on a membrane filter in order to achieve samples with sufficient total activity (Table 3).

2.4. Dissolution experiments

Two solutions, Gamble and Modified SLF, were applied to simulate human lung fluid. These kinds were often used in vitro in several studies of the solubility of radioactively contaminated aerosol particles [20,21]. The basic component of the aqueous solutions is NaCl. The freshly made solutions are alkalescent with a pH of 7.6 for Gamble and of 8.2 for Modified SLF. The chemical compositions are given in Table 2 together with two other well-known solutions.

The obtained filter fragments were covered with two membrane filters each, with a pore diameter of 0.22 μm, as a protection and were fixed in cartridges made of PTFE. The cartridges were placed in vessels of polyethylene, which were filled with 30 ml of freshly made SLF of one type. The vessels were kept at an ambient temperature of about 25 °C, which is a usual condition for in vitro dissolution tests with simulated lung fluid [14]. At several times up to 55 days after the beginning of the dissolution the SLF was changed. The activity of ^{137}Cs, ^{90}Sr, $^{239+240}$Pu and ^{241}Am was determined in each SLF sample. Further autoradiograms of the fragments were taken after the dissolution experiments.

2.5. Radiospectrometry measurements

The activities of ^{137}Cs and ^{241}Am on the filter fragments before and after the dissolution experiments and in the various samples of SLF were measured by gamma spectrometry. This was done with a high-purity germanium semiconductor gamma spectrometer GMX-30190-P-S (Ortec, 37.7% rel. efficiency) and a Walklab analyzer module (Silena). Filter samples were measured in a flat geometry, samples of SLF in a vial geometry.

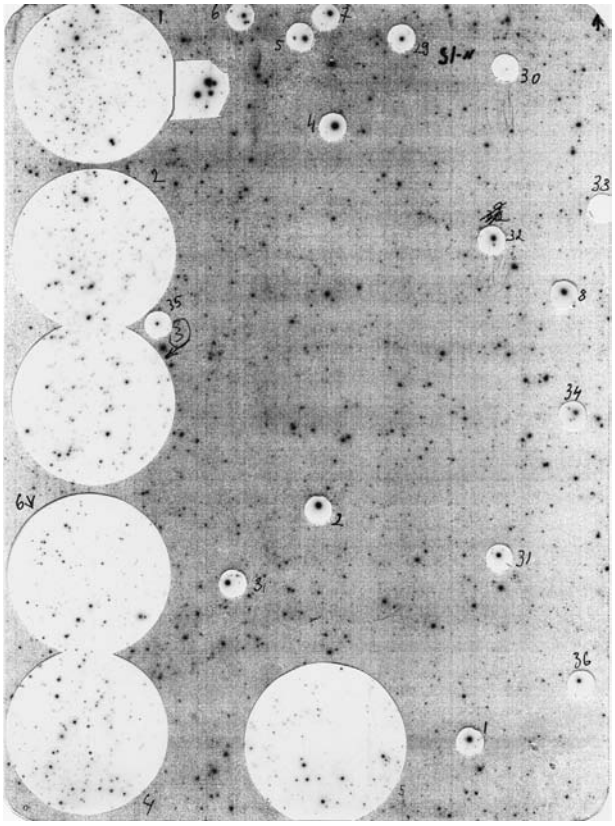

Fig. 1. Autoradiogram of a filter of sample type 2 with clearly visible dark spots of hot particles. The selected filter fragments with 48 and 8 mm diameter are marked as white circular areas.

Table 2
Composition of the simulated lung fluids (SLFs) Gamble, Modified SLF, serum ultrafiltrate stimulant (SUF) and Ringer's solution in mmol/l. The last two are taken from Aladova et al. [25] and are used in the discussion of the results.

	Gamble	Modified SLF	SUF	Ringer's solution
$CaCl_2 \cdot 6H_2O$	0.2	1.3	0.2	2
DTPA	–	–	0.2	–
Glycine	–	–	5	–
H_2SO_4	–	–	0.5	–
KCl	10	4	–	2
L-Cysteine	–	–	1	–
$MgCl_2$	27	1	–	–
NaAcetate	0.2	7	–	–
NaCitrate • 5 H_2O	1	0.3	0.2	–
NaCl	116	145	116	140
$NaHCO_3$	6	24	27	1
NH_4Cl	–	–	10	–
NaH_2PO_4	–	–	1.2	–
Na_2HPO_4 • $2H_2O$	1.2	1	–	–
Na_2SO_4	–	0.5	–	–
pH	7.6	8.2	7.4	7.4

After the gamma spectrometry measurements which followed the dissolution experiments, the activities of ^{90}Sr, ^{239}Pu and ^{240}Pu in the SLF samples and the filter fragments with the insoluble heels were measured by gross beta counting (alpha/beta counter LB 770-PC, Berthold) and alpha spectrometry (eight-channel alpha spectrometer Octete PC, Ortec Inc.), respectively. Because of their similar alpha-decay energies ^{239}Pu and ^{240}Pu cannot be distinguished spectrometrically. Therefore only the activity of both nuclides $^{239+240}$Pu together could be determined.

The mentioned measurement techniques required previous chemical treatment of the samples. The applied separation processes are described by Ageyev et al. [22]. Firstly, the filter fragments were ashed and the SLF samples were evaporated to dryness. Then, the samples were dissolved in 6 M HCl. Adding $Fe(OH)_3$ and aqueous solution of NH_3 yielded $Fe(OH)_3$ precipitation with Pu, other actinides and several other elements whereas Sr remained dissolved. Pu was transformed to Pu^{3+} by taking up the precipitation into 8 M HNO_3 and adding $NaNO_2$. It was separated from the other actinides in anion exchange resin AB-17 (NO_3^- form) by washing the resin firstly with 8 M HNO_3 and 10 M HCl to remove the other actinides and secondly with 9 M HCl and NH_4I, which eluted Pu. The eluted Pu was evaporated to dryness, taken up into $(NH_4)_2SO_4$ and electrodeposited on a metal plate, which was used in an alpha spectrometer.

Shortly before measurement the solved ^{90}Sr was separated from its decay product ^{90}Y in another $Fe(OH)_3$ precipitation, in which Sr stayed in the solution again. Then, it was precipitated as $SrCO_3$, whose gross beta activity was measured. During several weeks the activity of ^{90}Y grew until equilibrium with that of ^{90}Sr. Then the sample was measured a second time. From the activity of the first measurement only with ^{90}Sr and of the second one with both nuclides in equilibrium, the result could be corrected for the presence of other beta-emitting nuclides.

Chemical yields were determined from radionuclide tracers, which were added before the chemical treatment.

All uncertainties are calculated with a coverage factor $k=2$. Uncertainties of solubility fractions and rates are those from curve-fitting to the time-resolved measurement results.

3. Results and discussion

3.1. Total solubility

The fraction of the activity of hot particles which was dissolved into the SLF in a given time of several weeks is presented in Table 3. Important influencing parameters such as the sample type from Table 1, the type of SLF, the diameter of the hot particles (calculated either from their activity and known specific activity or from the stage in cascade impactor sampling) and the activity ratio of ^{137}Cs to $^{239+240}$Pu are given as well.

The samples differ from each other mainly in their ratio of the activities of ^{137}Cs to that of $^{239+240}$Pu. Some samples exceed the respective value of 61 for the nuclear fuel at ChNPP at the time of the measurements [10] significantly. These particles are likely to originate from vaporization, in which the more volatile Cs is enriched in comparison to Pu, and later condensation [23]. In contrast, hot particles on samples with a ^{137}Cs/$^{239+240}$Pu ratio close to 61 might consist of the original fuel matrix.

Fig. 2 demonstrates the impact of this activity ratio on the solubility: the solubility of ^{137}Cs features a strong increase with higher ^{137}Cs/$^{239+240}$Pu ratios, that of ^{90}Sr is slightly increased at higher activity ratios whereas that of $^{239+240}$Pu does not depend on the activity ratio. ^{137}Cs might be more soluble in condensation particles due to two effects: Firstly, in these particles it had become volatized before the origin of the particle and is now more loosely bound in the matrix of the particle. Secondly, the condensed ^{137}Cs is concentrated near the surface of the particle whereas in the particles which consist of the original fuel matrix it is distributed homogeneously throughout the volume of the particle. The three samples with extremely high ^{137}Cs/$^{239+240}$Pu ratios greater than 1000 consist of small hot particles which were sampled with the cascade impactor inside the Shelter.

No dependence of the dissolution of ^{137}Cs and ^{90}Sr on the two types of SLF could be observed (Fig. 2); the slopes of the regression lines are equal within their confidence intervals. Therefore, other studies which used one of these two simulated lung fluids [14,21] produced results which are comparable with each other. However,

Table 3
Dissolved fraction of ^{137}Cs, ^{90}Sr and $^{239+240}$Pu from hot particles into two types of SLF and influencing parameters. G stands for Gamble, M for Modified SLF.

Sample no.	Sample type	Average diameter [μm]	SLF	Beta activity [Bq]	^{137}Cs/$^{239+240}$Pu	Dissolution time [days]	Soluble fraction [%]		
							^{137}Cs	^{90}Sr	$^{239+240}$Pu
1	1	3.6	M	37	1320	35	38	5.8	2.2
2	1	1.9	M	43	1410	35	39	4.3	4.5
3	1	1.1	M	19	1120	35	36	4.4	1.8
4	2		G	127	152	35	66	8.0	0.41
5	2		G	118	173	35	58	9.6	0.62
6	2		G	96.9	168	35 (28 for Pu)	61	8.2	0.28
7	2	59.2	G	80.6	61.3	28	1.1	0.35	0.13
8	2	36.8	G	39.1	52.4	28	8	2.7	0.34
9	2	31.5	G	61.2	65.6	28	16	1.5	0.18
10	2	25	G	49.2	69	28	29	2.7	0.24
11	2		G	92.4	238	29	57	7.6	4.3
12	2		G	83.8	244	29	56	9.2	3.0
13	2		M	71	68	35	29	1.7	1.9
14	2		M	32	222	35	36	7.8	9
15	2		M	124	188	55	52	4.1	0.73
16	2		M	97.4	171	55	53	4.7	0.91
17	2		M	53.9	224	29	55	4.4	0.87
18	2	45.4	M	36.3	75	55 (29 for Cs)	3	0.41	–
19	2	28.6	M	45.6	87	29	22	1.3	0.2
20	2	27.3	M	39.6	41.9	29	39	1.3	0.39
21	2	15.9	M	22.4	149	29	43	4.1	0.9
22	2		M	34.5	281	28	34	4.6	0.39
23	2		M	19.5	171	28	24	3.4	0.3
24	2		M	19.1	122	28	35	4.2	0.44
25	2	30.4	M	43.9	58.3	28	2.8	0.82	0.08
26	2	20.8	M	36.4	50.5	28	13.5	0.42	0.05
27	2	11.4	M	29.9	62.1	28	22	0.83	0.07
28	3		G	75.9	119	29	18	8	0.34
29	3	55.4	G	399	53.8	29	1.6	0.18	0.04
30	3	41.9	G	326	38.3	29	0.9	0.21	0.05
31	3	20.0	G	66.9	58.8	29	20	13.2	0.11
32	3		M	175	69	35	3.5	2.2	1.3
33	3		M	114	72	35	1.6	1.2	0.53
34	4		G	20	30.4	28	3.6	0.76	0.26
35	4		G	12.5	43.4	28	3.9	3.4	0.17
36	4	30	G	32.7	32.1	28	3.2	2.1	0.46
37	4	19.6	G	31.8	30.9	28	1.2	2.2	0.43

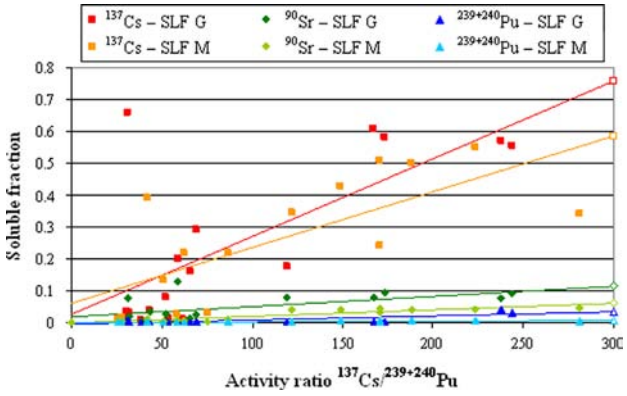

Fig. 2. Soluble fraction of ^{137}Cs, ^{90}Sr and $^{239+240}$Pu in Gamble (SLF G) and Modified SLF (SLF M). No obvious difference in the solubility into both types of SLF is observed. Lines of regression are marked with the symbol of the corresponding set of data points at the right-hand side of the diagram to guide the eye.

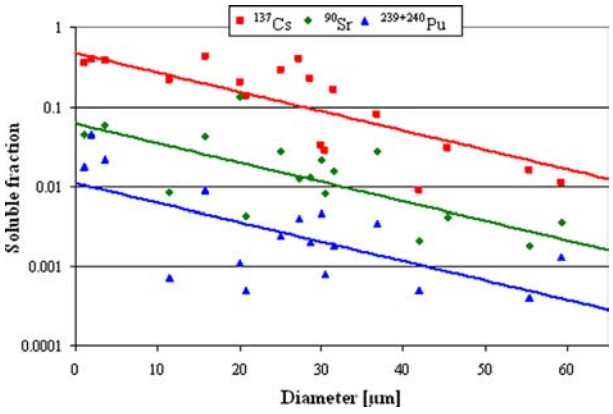

Fig. 3. Soluble fraction of ^{137}Cs, ^{90}Sr and $^{239+240}$Pu as a function of the diameter of the hot particles. Measured data points with fitted exponential functions (solid lines).

$^{239+240}$Pu dissolution was significantly stronger in Gamble SLF (slope $(10.8 \pm 3.6) \cdot 10^{-5}$) than in Modified SLF (slope $(2.6 \pm 1.0) \cdot 10^{-5}$).

The dissolved fraction as a function of the diameter of the hot particles is presented in Fig. 3. All investigated nuclides show a stronger solubility from smaller hot particles, with which a larger surface in comparison to the volume of the particle is available to dissolve from. Using an exponential model, the influence of the diameter d on the soluble fraction F can be described for

$$^{137}\mathrm{Cs}: F = 0.47\exp(-d/18\ \mu m)$$

$$^{90}\mathrm{Sr}: F = 0.061\exp(-d/18\ \mu m)$$

$$^{239+240}\mathrm{Pu}: F = 0.011\exp(-d/18\ \mu m)$$

Table 4
Parameters of the two-component model for the dissolution of ^{137}Cs into Gamble and Modified SLF. Values for samples 8–10 are based on only three data points each, for which reason no uncertainty can be given.

Sample number	Type of SLF (Gamble/Modified)	Rapidly soluble fraction f_r [%]	Characteristic times of dissolution	
			T_r [d]	T_s [d]
4	G	64.5 ± 2.4	6.71 ± 0.37	450 ± 280
5	G	56.6 ± 4.0	6.10 ± 0.71	710 ± 370
6	G	60.0 ± 1.2	6.51 ± 0.44	400 ± 270
7	G	2.0 ± 1.2	12.1 ± 7.2	> 10 000
8	G	7.8	9.0	> 10 000
9	G	18	10	> 10 000
10	G	31	11	> 10 000
11	G	48.5 ± 2.1	0.97 ± 0.13	140 ± 45
12	G	46.4 ± 2.3	0.96 ± 0.15	140 ± 47
15	M	49.0 ± 1.9	6.74 ± 0.42	590 ± 340
16	M	48.4 ± 2.8	7.7 ± 1.0	710 ± 300

Table 5
Parameters of the two-component model for the dissolution of ^{90}Sr into Gamble and Modified SLF.

Sample number	Type of SLF (Gamble/Modified)	Rapidly soluble fraction f_r [%]	Characteristic times of dissolution	
			T_r [d]	T_s [d]
4	G	9.7 ± 2.4	10.1 ± 3.2	> 3000
5	G	10.78 ± 0.45	13.2 ± 1.3	> 1000
6	G	12.10 ± 0.35	9.7 ± 1.3	> 1000
11	G	6.74 ± 0.46	0.89 ± 0.15	2500 ± 1800
12	G	8.23 ± 0.38	0.76 ± 0.12	2500 ± 1200
15	M	3.62 ± 0.23	3.34 ± 0.94	7000 ± 3000
16	M	4.23 ± 0.17	4.03 ± 0.40	8000 ± 3200
20	M	1.11 ± 0.30	9.6 ± 2.1	14 000 ± 8000
21	M	3.56 ± 0.32	5.2 ± 1.2	5000 ± 2000

Table 6
Parameters of the two-component model for the dissolution of $^{239+240}$Pu into Gamble and Modified SLF.

Sample number	Type of SLF (Gamble/Modified)	Rapidly soluble fraction f_r [%]	Characteristic times of dissolution	
			T_r [d]	T_s [d]
4	G	0.415 ± 0.052	8.1 ± 3.2	> 10 000
5	G	0.300 ± 0.016	8.0 ± 1.4	> 10 000
6	G	0.635 ± 0.034	5.1 ± 1.3	> 10 000
11	G	4.09 ± 0.22	0.384 ± 0.083	6000 ± 3200
12	G	3.00 ± 0.20	1.03 ± 0.30	> 10 000
15	M	0.702 ± 0.059	5.6 ± 1.6	> 10 000
16	M	0.94 ± 0.12	6.6 ± 1.2	> 10 000

3.2. Time-resolved dissolution

Mercer described the dissolution of particles in a fluid by a first-order kinetics equation [24]. He derived this for a population of spherical particles having initially a log-normal size distribution; the mass M which is not dissolved at time t can be calculated as

$$M/M_0 = f_1 \exp(-\lambda_1\beta) + f_2 \exp(-\lambda_2\beta) \quad (2)$$

where M_0 is the initial mass of the population of particles and β is a dimensionless time variable; f_i and λ_i are functions only of the geometric standard deviation of the size distribution and $f_1+f_2=1$. If a constant specific activity of radioactive particles can be assumed, Eq. (2) can be written in terms of the activity A and can be applied to the undissolved fraction $F=A(t)/A_0$ at time t by multiplication of M and M_0 with the specific activity:

$$F(t) = A/A_0 = f_r \exp(-t/T_r) + f_s \exp(-t/T_s) \quad (3)$$

where the coefficients f_r and f_s (dimensionless) are the rapidly and slowly soluble fractions; $f_r+f_s=1$. T_r and T_s are the characteristic times of dissolution; their reciprocal values are called dissolution rates.

Tables 4–7 give the rapidly and slowly soluble fractions as well as the respective characteristic times as the parameters of the

Table 7
Parameters of the two-component model for the dissolution of ^{214}Am into Gamble and Modified SLF.

Sample number	Type of SLF (Gamble/Modified)	Rapidly soluble fraction f_r [%]	Characteristic times of dissolution	
			T_r [d]	T_s [d]
4	G	0.69 ± 0.42	13.6 ± 6.2	6000 ± 4000
5	G	0.718 ± 0.051	10.9 ± 2.2	> 20 000
6	G	1.07 ± 0.37	20 ± 12	> 20 000
11	G	0.804 ± 0.057	0.98 ± 0.22	11 000 ± 3800
12	G	0.475 ± 0.040	1.85 ± 0.39	14 600 ± 4200
15	M	0.63 ± 0.11	15.7 ± 6.4	> 20 000
16	M	0.611 ± 0.014	9.97 ± 0.79	> 20 000
20	M	0.539 ± 0.095	15.1 ± 5.8	> 20 000
21	M	0.806 ± 0.087	10.5 ± 3.4	> 20 000

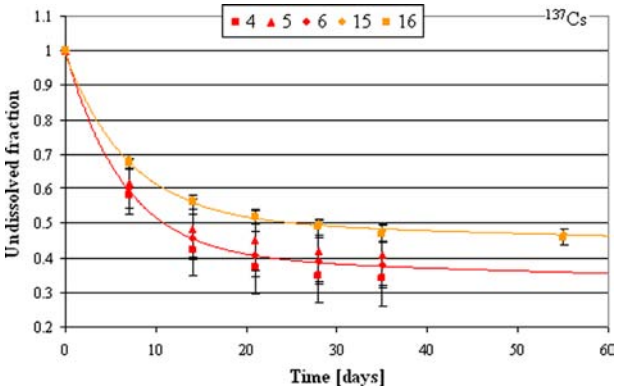

Fig. 4. Activity of undissolved ^{137}Cs as a function of time for selected samples of type 2. Samples 4–6: Gamble SLF, samples 15 and 16: Modified SLF. Data points: measured values, solid line: fitted result of the two-component exponential model, averaged for samples 4–6, 15 and 16.

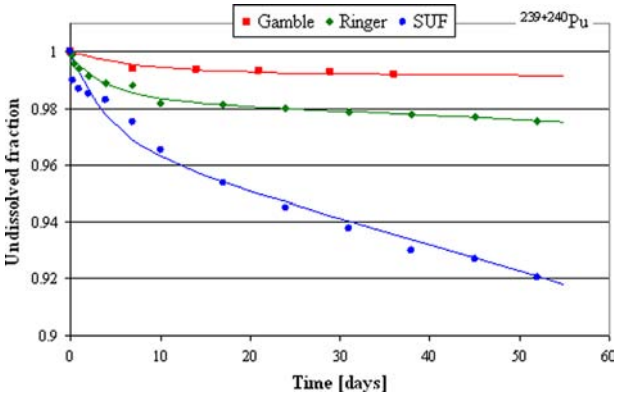

Fig. 5. Comparison of the solubility of plutonium oxide into serum ultrafiltrate stimulant (SUF) and Ringer's solution (both at pH 7.4), which are used as simulated lung fluids as well (data taken from [25]), and $^{239+240}$Pu from samples 4–6, 15 and 16 into Gamble solution.

Table 8
Dose coefficients for the inhalation of nuclear fuel particles from Chernobyl with a diameter of 20 μm by reference workers at light work and at heavy work (effective dose coefficients only), calculated with the computer software IMBA [26] and the given f_1 value. Dose coefficients with reference values are shown for comparison for light work (taken from ICRP 68) and for heavy work (calculated with IMBA).

		^{137}Cs	^{90}Sr	$^{239+240}$Pu	^{241}Am
f_1		1	0.3	0.00001	0.0005
Reference absorption type		F	F	S (insoluble oxides)	M
Organ		Dose coefficients [Sv/Bq]			
Respiratory tract	ET	2.5×10^{-8}	6.7×10^{-8}	7.4×10^{-5}	7.2×10^{-5}
	ET1	1.8×10^{-6}	2.0×10^{-6}	1.4×10^{-6}	2.7×10^{-5}
	ET2	2.3×10^{-8}	6.4×10^{-8}	7.3×10^{-5}	7.2×10^{-5}
	LN(ET)	1.5×10^{-8}	4.1×10^{-7}	2.8×10^{-4}	1.8×10^{-4}
	BBsec	3.5×10^{-8}	1.0×10^{-7}	2.4×10^{-5}	3.0×10^{-5}
	BBbas	3.0×10^{-8}	9.2×10^{-8}	2.2×10^{-6}	3.5×10^{-6}
	bb	1.2×10^{-8}	7.1×10^{-8}	7.7×10^{-6}	8.1×10^{-6}
	AI	1.0×10^{-8}	7.3×10^{-8}	1.3×10^{-5}	1.1×10^{-5}
	LN(TH)	8.0×10^{-9}	1.5×10^{-7}	2.4×10^{-4}	1.5×10^{-4}
	Lung	1.8×10^{-8}	8.0×10^{-8}	1.1×10^{-5}	1.2×10^{-5}
Urinary bladder		5.1×10^{-9}	5.3×10^{-10}	1.3×10^{-9}	2.1×10^{-8}
Breast		4.1×10^{-9}	2.4×10^{-10}	1.3×10^{-9}	2.1×10^{-8}
Gall bladder		4.9×10^{-9}	2.4×10^{-10}	1.3×10^{-9}	2.1×10^{-8}
Brain		4.2×10^{-9}	2.4×10^{-10}	1.3×10^{-9}	2.1×10^{-8}
Skin		3.8×10^{-9}	2.4×10^{-10}	1.3×10^{-9}	2.1×10^{-8}
Heart wall		5.1×10^{-9}	2.4×10^{-10}	1.3×10^{-9}	2.1×10^{-8}
Testes		4.4×10^{-9}	2.4×10^{-10}	9.6×10^{-9}	2.5×10^{-7}
Gonads		5.1×10^{-9}	2.4×10^{-10}	9.6×10^{-9}	2.5×10^{-7}
Bone surface		4.9×10^{-9}	1.5×10^{-7}	7.2×10^{-7}	1.3×10^{-5}
Liver		4.9×10^{-9}	2.4×10^{-10}	1.5×10^{-7}	8.4×10^{-7}
Gastrointestinal tract	Esophagus	4.8×10^{-9}	2.4×10^{-10}	1.3×10^{-9}	2.1×10^{-8}
	Stomach	4.8×10^{-9}	3.3×10^{-10}	1.7×10^{-9}	2.1×10^{-8}
	Small intestine	5.2×10^{-9}	4.2×10^{-10}	2.3×10^{-9}	2.2×10^{-8}
	Upper large intestine	5.1×10^{-9}	2.1×10^{-9}	7.6×10^{-9}	2.8×10^{-8}
	Lower large intestine	5.8×10^{-9}	7.9×10^{-9}	2.0×10^{-8}	4.1×10^{-8}
	Colon	5.4×10^{-9}	4.6×10^{-9}	1.3×10^{-8}	3.4×10^{-8}
Spleen		4.8×10^{-9}	2.4×10^{-10}	1.3×10^{-9}	2.1×10^{-8}
Muscle		4.5×10^{-9}	2.4×10^{-10}	1.3×10^{-9}	2.1×10^{-8}
Adrenals		5.1×10^{-9}	2.4×10^{-10}	1.3×10^{-9}	2.1×10^{-8}
Kidneys		4.8×10^{-9}	2.4×10^{-10}	2.9×10^{-9}	7.0×10^{-8}
Ovaries		5.1×10^{-9}	2.4×10^{-10}	9.4×10^{-9}	2.5×10^{-7}
Pancreas		5.2×10^{-9}	2.4×10^{-10}	1.3×10^{-9}	2.1×10^{-8}
Remainder		1.5×10^{-8}	2.7×10^{-10}	3.7×10^{-5}	3.6×10^{-5}
Red bone marrow		4.7×10^{-9}	6.3×10^{-8}	3.4×10^{-8}	4.6×10^{-7}
Thyroid		4.7×10^{-9}	2.4×10^{-10}	1.3×10^{-9}	2.1×10^{-8}
Thymus		4.8×10^{-9}	2.4×10^{-10}	1.3×10^{-9}	2.1×10^{-8}
Uterus		5.1×10^{-9}	2.4×10^{-10}	1.3×10^{-9}	2.1×10^{-8}
Effective		7.0×10^{-9}	2.0×10^{-8}	3.2×10^{-6}	3.6×10^{-6}
Effective dose coefficients from ICRP 68 [27]		6.7×10^{-9}	3.0×10^{-8}	8.3×10^{-6}	2.7×10^{-5}
Individual effective dose coefficients for heavy work		8.3×10^{-9}	1.8×10^{-8}	3.3×10^{-6}	3.7×10^{-6}
Reference effective dose coefficients for heavy work		7.0×10^{-9}	3.2×10^{-8}	9.8×10^{-6}	2.9×10^{-5}

two-component exponential model for the dissolution of ^{137}Cs, ^{90}Sr, $^{239+240}$Pu and ^{241}Am as a function of time. Fig. 4 presents exemplary data for ^{137}Cs; for better perceptibility, error bars are drawn only for some data sets.

Dissolution of a certain activity fraction of the hot particles within the first few days can be observed for all three investigated nuclides. Only the amount which is soluble within this first time differs between the nuclides. The remaining fraction features very slow solubility. With a characteristic time for bronchial clearance (transport from the bronchi to the pharynx) of several hours [15] a significant part of the deposited activity will be dissolved and can thus be subjected to transport into the blood.

3.3. Comparison with solubility studies of industrial plutonium aerosol

Aladova et al. presented results of dissolution experiments of plutonium from nuclear industrial aerosols from the Production Association Mayak in different simulated lung fluids (Table 2, [25]). Fig. 5 shows that the hot particles are dissolved very slowly into Gamble solution in comparison to the plutonium oxide into Ringer's solution and even more into SUF. Comparing the chemical structure of the solutions used as simulated lung fluids the following can be noted:

- The basic component of all solutions is NaCl.
- Ringer's solution has the least difficult salt structure (7.4 g/l) and practically does not contain complexing ligands.
- All solutions are alkalescent. Ringer's solution and SUF have a pH of 7.4, Gamble has a pH of 7.6 and Modified SLF of 8.2.

3.4. Implications for inhalation dosimetry

The applied model of time-resolved solubility, which comprises two exponential contributions with different constant dissolution rates, conforms to the model of time-resolved uptake of radionuclides into the blood, which is part of the Human Respiratory Tract Model of the ICRP. The dissolution rates $1/T_r$ and $1/T_s$ correspond to the rates s_r and s_s of rapid and of slow solubility, respectively. Thus, the parameters which were determined for the solubility of the studied radionuclides from hot particles can be applied for the calculation of inhalation dose coefficients which are specific for the exposure to these hot particles as it can occur

during the construction of the new Chernobyl shelter. Such a calculation of dose coefficients from individual parameters is explicitly recommended [15].

Dose coefficients were calculated using the computer software IMBA, which was developed by the Health Protection Agency of the UK [26]. They are presented in Table 8 for a reference worker according to ICRP 68 [27] (normal nose-breathing adult male at light work). The dose coefficient for the effective dose is presented also for a reference worker at heavy work instead of light work (7 h light exercise, 1 h heavy exercise per day as defined in [15]). As further input parameters a density of 10.4 g/cm³ [19] and the f_1 value of solubility in the gastrointestinal tract from ICRP 68 [27] for the respective nuclide were assumed. Reference values for the respective nuclide were used for the transport rates in the respiratory tract and in the gastro-intestinal tract as well as for the biokinetic transfer rates. The diameter of the hot particles was assumed as 20 μm, which is approximately the mode value of the diameter distribution of the hot particles investigated in this study. At even larger diameters of 60 μm, the solubilities of ^{137}Cs, ^{90}Sr and $^{239+240}$Pu are about one order of magnitude smaller than those at 20 μm; however, the deposition in the thoracic parts of the respiratory tract is smaller by about one order of magnitude [15].

Due to their slow solubility, all studied nuclides cause greater organ doses in the respiratory tract and smaller doses in the other organs compared to ICRP standard values [27]. The effective dose coefficient of ^{241}Am is smaller by almost one order of magnitude and that of $^{239+240}$Pu is smaller by a factor of about 2.5 compared to the respective standard dose coefficient for workers. The effective dose coefficient of ^{90}Sr is about 2/3 and that of ^{137}Cs is about the same as compared to the respective standard dose coefficients. Both the individually calculated and the reference effective dose coefficients for heavy work are close to those for light work.

Acknowledgment

This study was supported by the German Federal Ministry for the Environment, Nature Conservation and Nuclear Safety (BMU) under Contract StSch 4544. Its contents are solely the responsibility of the authors.

References

[1] U.S. Environmental Protection Agency, Health Effects of Alpha-Emitting Particles in the Respiratory Tract, National Academy of Sciences, Washington, DC, 1976.
[2] A.P. Ermilov, A.M. Ziborov, Radiat. Risk 3 (1993) 134–138, in Russian.
[3] Y.V. Dubasov, V.G. Savonenkov, E.A. Smirnova, Radiochemistry 38 (1996) 101–116, in Russian.
[4] F.J. Sandalls, M.G. Segal, N. Victorova, J. Environ. Radioact. 18 (1993) 5–22.
[5] V. Zheltonozhsky, K. Mück, M. Bondarkov, J. Environ. Radioact. 57 (2001) 151–166.
[6] B. Salbu, T. Krekling, D.H. Oughton, Analyst 123 (1998) 843–849.
[7] Ukrainian Institute of Agricultural Radiology, Hot Particles Database, Microsoft Access Database, Kiev, 2001.
[8] R. Pöllänen, I. Valkama, H. Toivonen, Atmos. Environ. 31 (1997) 3575–3590.
[9] F. Wagenpfeil, J. Tschiersch, J. Environ. Radioact. 52 (2001) 5–16.
[10] R.G. Cuddihy, G.L. Finch, F.F. Hahn, J.A. Mewhinney, S.J. Rothenberg, D. A. Powers, Environ. Sci. Technol. 23 (1989) 89–95.
[11] C.A. Bogatov, A.A. Borovoi, Y.V. Dubasov, V.V. Lomonosov, At. Energy 69 (1990) 595–601.
[12] V.A. Kutkov, O.I. Kamarinskaya, Proceedings of 9th IRPA International Congress on Radiation Protection, Vienna, 1996, 445–447 pp.
[13] E.K. Garger, A.D. Sazhenyuk, A.A. Odintzov, H.G. Paretzke, P. Roth, J. Tschiersch, Radiat. Environ. Biophys. 43 (2004) 43–49.
[14] E. Ansoborlo, M.H. Hengé-Napoli, V. Chazel, R. Gibert, R.A. Guilmette, Health Phys. 77 (1999) 638–645.
[15] International Commission on Radiological Protection, Human Respiratory Tract Model for Radiological Protection, ICRP Publication 66, Pergamon, Oxford, 1994.
[16] E.K. Garger, B.L. Gorkovenko, V.K. Shinkarenko, Probl. Nucl. Power Plants Saf. Chernobyl 2 (2005) 33–40, in Russian.
[17] V.K. Shynkarenko, Probl. Nucl. Power Plants Saf. Chernobyl 9 (2008) 103–139, in Russian.
[18] International Commission on Radiological Protection, Guide for the Practical Application of the ICRP Human Respiratory Tract Model, ICRP Supporting Guidance 3, Pergamon, Oxford, 2002.
[19] V.A. Kashparov, Y.A. Ivanov., S.I. Zvarisch, V.P. Protsak, Y.V. Khomutinin, A.D. Kurepin, E.M. Pazukhin, Nucl. Technol. 114 (1996) 246–252.
[20] V.A. Kashparov, V.I. Yoschenko, S.I. Zvarich, V.P. Protsak, E.M. Pazukhin, Radiochemistry 39 (1997) 77–79.
[21] A.F. Eidson, W.C. Griffith, Health Phys. 46 (1984) 151–163.
[22] V.A. Ageyev, O.O. Odintsov, A.D. Sajeniouk, J. Radioanal. Nucl. Chem. 264 (2005) 337–342.
[23] Nuclear Energy Agency, Chernobyl: Assessment of Radiological and Health Impact—2002 Update of Chernobyl: Ten Years On, OECD Publications, Paris, 2002.
[24] T.T. Mercer, Health Phys. 13 (1967) 1211–1221.
[25] E.E. Aladova, S.A. Romanov, R.A. Guilmette, V.F. Khokhryakov, K.G. Suslova, Radiat. Prot. Dosim. 127 (2007) 60–63.
[26] Health Protection Agency, IMBA Professional (GSF Edition), version 3.0, 2003.
[27] International Commission on Radiological Protection, Dose Coefficients for Intakes of Radionuclides by Workers, ICRP Publication 68, Pergamon, Oxford, 1994.